Chapter 8

Posterior fossa abnormalities in high-risk term infants: comparison of ultrasound and MRI

Sylke J. Steggerda
Francisca T. de Bruïne
Vivianne E.H.J. Smits-Wintjens
Paula Verbon
Frans J. Walther
G. van Wezel-Meijler

Submitted

Abstract

Purpose: To assess the frequency and characteristics of posterior fossa (PF) abnormalities in a cohort of high-risk term neonates and the diagnostic performance of cranial ultrasound (CUS) with additional mastoid fontanelle (MF) views for the detection of these abnormalities, with magnetic resonance imaging (MRI) being the reference diagnostic standard.

Materials and Methods: The ethics committee waived the need for informed consent for this study. In this retrospective cohort study 113 term neonates with CUS and subsequent MRI were included. Sensitivity, specificity, positive predictive value and negative predictive value of routine CUS and CUS with MF views were calculated.

Results: PF abnormalities were diagnosed on CUS in 46 of the 113 infants. MRI confirmed these findings in 43 and showed additional abnormalities in 32 infants. The sensitivity and specificity of anterior fontanelle views for major PF abnormalities as seen on MRI were 16% and 99%. Adding MF views increased the sensitivity of US to 82%. The sensitivity and specificity of MF views for the detection of any (major or minor) PF abnormality were 57% and 95% respectively. Especially acute hypoxic-ischemic injury of the cerebellar vermis and small subdural and punctate cerebellar hemorrhage remained undetected by CUS.

Conclusion: PF abnormalities are frequent in high-risk term infants. MF-CUS enables early diagnosis of the majority of major and clinically relevant PF abnormalities. We therefore propagate to routinely perform MF-CUS in high-risk term neonates.

Introduction

The nowadays widespread availability of advanced neuroimaging techniques leads to increased detection of cerebellar injury and other posterior fossa (PF) abnormalities in newborn infants requiring intensive care. Cerebellar injury is an important complication of preterm birth and may also occur in full-term infants (1,2).

In full-term infants cerebellar and extra axial PF hemorrhage are associated with traumatic delivery, perinatal infection, supratentorial hemorrhage and perinatal asphyxia (2-4). The cerebellum can be involved in hypoxic-ischemic injury because granule cell neurons and Purkinje cells are vulnerable in the full-term neonate (5). Cerebellar abnormalities are frequently reported in neonates with metabolic disorders (6,7) and congenital PF malformations are common in neonates with other central nervous system (CNS) abnormalities.

Cerebellar abnormalities are associated with a broad spectrum of neurodevelopmental disabilities (2). Early detection is therefore important. Cranial ultrasound (CUS) is the primary neonatal neuroimaging technique. It can be performed early and repeatedly at the bedside and provides instant diagnostic information. CUS is traditionally performed through the anterior fontanelle (AF). This enables reliable views of supratentorial structures, but visualization of the PF is less optimal due to its distance away from the transducer (8). In addition, the echogenic tentorium and vermis may impede visualization. The mastoid fontanelle (MF) enables a better view of the PF (8-11). In a previous study (12) we showed that addition of MF views in preterm infants improved detection of cerebellar injury as compared to CUS with only AF views. Despite the clinical importance of cerebellar injury and other PF abnormalities, MF views are often not included in the CUS examination of the brain of high-risk term infants.

The posterior fossa is well depicted at MRI. However, compared with CUS, MRI is a burdensome procedure in critically ill neonates and less suitable for early or serial imaging.

The aims of this study were to assess: (1) the frequency and characteristics of PF abnormalities in a cohort of high-risk term neonates, and (2) the diagnostic performance of CUS with additional MF views (MF-CUS) for the detection of these abnormalities with MRI being the reference diagnostic standard.

Materials and Methods

Patients

The ethics committee of the Leiden University Medical Center waived the need for informed consent for this retrospective study. A systematic database search identified all term infants (gestational age >36 weeks) admitted to the neonatal unit of the Leiden University Medical Center (tertiary neonatal referral center) between January 2008 and December 2012 with a diagnosis of hypoxic-ischemic encephalopathy (HIE), CNS infection, supratentorial intracranial hemorrhage, ventricular dilatation, metabolic disorder, congenital CNS malformation and/or abnormal neurologic examination (3). Infants were eligible for the study if they had undergone at least one good quality CUS scan that included both AF and MF views and at least one MRI examination during admission.

We included 113 infants with a total of 187 CUS examinations (mean number of CUS scans 1.7 per patient (range 1-7)) and 117 MR examinations. Patient characteristics are shown in Table 1.

CUS

CUS was performed by an experienced neonatologist or fellow-neonatologist, using an US system with multifrequency (5-10 MHz) transducers (Aloka Alpha 10; Biomedic Nederland BV, Almere, The Netherlands). Our standard CUS protocol includes imaging through the AF in at least six coronal and five sagittal planes (13). Standard transducer frequency is set at 7.5 MHz. To assess deeper structures, including the posterior fossa, a frequency of 5 MHz can be applied. The CUS protocol includes at least one examination with additional MF views in term neonates who are considered at risk for PF abnormalities (neonates with HIE, CNS infection, intracranial hemorrhage, ventricular dilatation, metabolic disorder, congenital CNS malformation and/or abnormal neurologic examination) (3). Scanning through the MF is performed in axial and coronal planes, with views of the ventricular system, brain stem, cerebellar peduncles, vermis, and hemispheres (8,10,13). Generally one of the MF is used, depending on the position of the infant. When abnormalities are suspected, additional images can be obtained using the opposite MF.

All CUS scans that included both AF and MF views were reviewed by at least two investigators (G.M., S.J.S. and V.E.H.J.S.W. with 25 and 10 years of experience in

Table 1. Patient characteristics (*n*=113)

Gestational age (weeks)*	38.8 ± 1.7
Birth weight (grams)*	3280 ± 679
Male gender	61 (54)
Mode of delivery	
- Spontaneous birth	46 (41)
- Vacuum/forceps assisted	22 (20)
- Elective caesarean section	18 (16)
- Emergency caesarean section	27 (24)
Apgar score 5 min#	5.8 (0-10)
Died	22 (20)
High risk category:	
- HIE	51 (45)
- Hemorrhage	10 (9)
- Traumatic delivery	4 (4)
- CNS infection	5 (4)
- Metabolic disorder	8 (7)
- Congenital malformation	18 (16)
- Other	17 (15)
Age at MF-CUS (days)*	5.4 ± 5.0
Age at MRI (days)*	8.0 ± 8.8
- Cases with HIE (days)*	6.3 ± 1.4
Number of MF-cUS#	1.7 (1-7)

HIE=hypoxic-ischemic encephalopathy, CNS=central nervous system, MF-CUS=mastoid fontanel cranial ultrasound. Except when indicated, data are number of infants with percentages in parentheses.
*mean ± standard deviation # mean with range in parentheses.

CUS) for the presence of PF malformation, loss of normal anatomic features, local or diffuse echogenicity changes in the cerebellar parenchyma (hemispheres and/or vermis), abnormalities in size and/or shape of the fourth ventricle, echogenicity within the fourth ventricle and abnormalities in other PF structures (cisterna magna, subarachnoid and subdural spaces).

To prevent recall bias, CUS scans were reviewed at least 4 months after they were made. The investigators were blinded to the patients' names, clinical history and MRI results and reviewed the scans together. Any discrepancies were solved by consensus.

MRI

In our hospital, MRI examination of the brain (Achieva 3T; Philips Medical Systems, Best, The Netherlands) is performed in all neonates with clinical or CUS suspicion of parenchymal brain abnormalities. Details of the MRI procedure and scanning protocols have been reported previously (14). A standard MRI examination includes a 3D T1-weighted turbo field-echo sequence (repetition time [TR] 9.7ms, echo time [TE] 4.6ms, flip angle 8°, field of view [FOV] 180mm, slice thickness 1mm, no gap), a T2-weighted turbo spin-echo sequence (TR 6269ms, TE 120ms, turbo factor 18, FOV 180mm, slice thickness 2mm), a T2* fast field-echo sequence (TR 735ms, TE 16ms, flip angle 18°, FOV 230mm, slice thickness 4mm) and diffusion-weighted spin-echo sequences in three directions (TR 2406ms, TE 64ms, FOV 180mm, slice thickness 4mm, b-value 1000s/mm^2).

All MRI scans were reviewed by two experienced investigators (F.T.d.B., pediatric neuroradiologist with 20 years of experience and S.J.S with 10 years of experience in neonatal MRI). To avoid recall bias, this was done at least 6 weeks after the CUS scans were reviewed. The investigators were blinded to the patients' names, clinical history and CUS findings and reviewed the scans together. Any discrepancies in interpretation were resolved by consensus. MRI scans were reviewed for: presence of PF malformation, hemorrhagic lesions on T2 and/or T2* sequences, more diffuse signal intensity (SI) changes on T1-,T2-, and/or diffusion-weighted images in the cerebellar parenchyma (hemispheres and/or vermis), abnormalities in size and/or shape of the fourth ventricle, hemorrhage in the fourth ventricle and PF extra axial hemorrhage. If abnormalities were present, location and extent were noted and whether these were visible on T1- and/or T2-, or only on T2* or diffusion-weighted images.

The following CUS and MRI abnormalities were considered major and clinically relevant: PF malformation, large cerebellar hemorrhage (>4 mm), diffuse echogenicity or SI changes in the cerebellar parenchyma, large extra axial hemorrhage with mass effect, and fourth ventricular dilatation or compression. Other abnormalities, such as mild enlargement of the cisterna magna with an intact vermis and without other structural abnormalities or mass effect, punctate cerebellar hemorrhage (<4 mm), and small subdural or subarachnoid hemorrhage without mass effect were considered minor and less relevant (15-17).

Data analysis

Statistical analysis was performed using SPSS software (SPSS 17; Chicago, Illinois, USA). The frequency of PF abnormalities on CUS and MRI was calculated. We compared the diagnostic performance of CUS for the detection of PF abnormalities with the results of MRI, which was considered the reference standard. We calculated sensitivity, specificity, positive predictive value and negative predictive value of CUS with and without MF views.

Results

CUS

In 46 (41%) of the 113 infants CUS detected abnormalities in the PF. In 39 (85%) of 46 infants these abnormalities were only seen on MF views. In 6 infants (13%) abnormalities were seen on both AF and MF views and in 1 infant (2%) only on AF views.

MRI

MRI was performed at a mean age of 8.0 days (SD ± 8.8). Mean interval between MF CUS and MRI was 3.1 days (SD ± 7.9). In 75 (66%) of the 113 infants MRI depicted abnormalities in the PF.

Comparison CUS and MRI

MRI findings in infants with abnormal CUS

In 43 (96%) of 45 infants the PF abnormalities on MF-CUS were confirmed by MRI. In 31 infants the abnormalities were classified as major and clinically relevant (Table 2), including 2 infants with a large extra axial hemorrhage, 2 with a large cerebellar hemorrhage and 3 with a hemorrhagic clot in the fourth ventricle and post-hemorrhagic ventricular dilatation (Figure 1). In 9 infants with HIE, in whom MF-CUS showed echogenicity changes of the cerebellar vermis and/or hemispheres, MRI showed SI changes on T1- /T2- and/or diffusion-weighted images (Figure 2). In 2 of these cases, MRI showed additional small hemorrhagic lesions in the cerebellar parenchyma. In 3 infants with CNS infection, PF abnormalities were seen on both MF-CUS and MRI (Figure 3). There were 6 cases with cerebellar hypoplasia (Figure 4), in 5 of them a metabolic disorder was diagnosed (Table 2). Six infants had other major PF malformations diagnosed on both MF-CUS and MRI.

Table 2. Imaging findings in infants with major abnormalities on mastoid fontanelle cranial ultrasound (MF-CUS)

Infant	GA	Category	MF-CUS
1	39	HIE	Increased echogenicity cerebellar vermis and hemispheres
2	40	HIE	Large hemorrhage cerebellar vermis and hemispheres, small SDH
3	36	HIE	Increased echogenicity cerebellar vermis and hemispheres
4	41	HIE	Increased echogenicity cerebellar vermis and hemispheres, loss of foliation
5	39	HIE	Increased echogenicity cerebellar vermis and hemispheres, loss of foliation
6	37	HIE	Increased echogenicity cerebellar vermis and hemispheres, loss of foliation
7	41	HIE	Increased echogenicity cerebellar hemispheres, loss of foliation, possible posterior fossa cyst
8	38	HIE	Increased echogenicity cerebellar vermis and hemispheres, loss of foliation
9	40	HIE	Increased echogenicity cerebellar hemispheres, loss of foliation
10	41	HIE	Increased echogenicity cerebellar vermis and hemispheres, loss of foliation
11	40	CNS infection	Increased echogenicity cerebellar vermis and hemispheres
12	40	CNS infection	Subdural debris and strands, dilated fourth ventricle with debris
13	37	CNS infection	Increased echogenicity cerebellar vermis and hemispheres, loss of foliation
14	40	Metabolic disorder	Cerebellar hypoplasia, posterior fossa cyst
15	37	Metabolic disorder	Cerebellar hypoplasia
16	38	Metabolic disorder	Cerebellar hypoplasia
17	36	Metabolic disorder	Cerebellar hypoplasia
18	38	Other	Cerebellar hypoplasia
19	36	Malformation	Posterior fossa cyst, compression vermis and left cerebellar hemisphere
20	38	Malformation	Cerebellar hypoplasia, enlarged fourth ventricle
21	37	Malformation	Small posterior fossa, compressed cerebellum and fourth ventricle
22	40	Malformation	Small posterior fossa, compressed cerebellum
23	41	Malformation	Posterior fossa cyst
24	38	Malformation	Loss of anatomic features, fourth ventricle not visible
25	38	Malformation	Small, compressed fourth ventricle
26	41	Hemorrhage	Echogenic clot in dilated fourth ventricle, small SDH
27	38	Hemorrhage	Echogenic clot in dilated fourth ventricle
28	40	Hemorrhage	Echogenic clot in dilated fourth ventricle
29	39	Other	Large extra axial hemorrhage with mass effect on right cerebellar hemisphere and fourth ventricle
30	37	Other	Large extra axial haemorrhage with mass effect on cerebellar vermis, hemispheres and fourth ventricle
31	37	Other	Disruption/atrophy of cerebellar vermis and hemispheres
32	40	CNS infection	Increased echogenicity both hemispheres and loss of foliation

GA=gestational age, HIE=hypoxic-ischemic encephalopathy, CNS=central nervous system, SI-=signal intensity.

MRI	Other diagnoses
Abnormal SI cerebellar vermis and hemispheres, small SDH	
Large hemorrhage cerebellar vermis and hemispheres, small SDH	Supratentorial ventricular dilatation
Abnormal SI cerebellar vermis and hemispheres, punctate hemorrhages	
Abnormal SI cerebellar vermis and hemispheres Single small cerebellar hemorrhage	Died
Abnormal SI cerebellar vermis and hemispheres	Died
Abnormal SI cerebellar vermis and hemispheres	Died
Abnormal SI cerebellar vermis and hemispheres, arachnoid cyst	Died
Abnormal SI cerebellar vermis	Died
Abnormal SI cerebellar vermis and hemispheres	Died
Abnormal SI cerebellar vermis and hemispheres	
Abnormal SI cerebellar vermis and hemispheres, small SDH	Group B streptococcal meningitis
Subdural debris and strands, dilated fourth ventricle with debris	E. Coli meningitis, ventricular dilatation neurosurgical intervention
Abnormal SI both cerebellar hemispheres, subdural empyema	Pneumococcal meningitis, ventricular dilatation neurosurgical intervention
Cerebellar hypoplasia, posterior fossa arachnoid cyst	Pyruvate dehydrogenase complex deficiency
Cerebellar hypoplasia	Adenylsuccinate lyase deficiency, died
Cerebellar hypoplasia	3-methylglutaconic aciduria, died
Cerebellar hypoplasia	Mitochondrial disease, died
Cerebellar hypoplasia, abnormal SI hemispheres	Suspected metabolic disorder, died
Arachnoid cyst, compression vermis, left hemisphere	Neurosurgical intervention
Cerebellar hypoplasia, enlarged fourth ventricle	Trisomy 21, died
Compressed cerebellum and fourth ventricle	Hydrocephalus, supratentorial cyst, neurosurgical intervention
Small posterior fossa, compressed cerebellum	Hydrocephalus, neurosurgical intervention
Arachnoid cyst, compression of cerebellar vermis	Hydrocephalus, neurosurgical intervention
Displacement posterior fossa structures	Posterior encephalocele, died
Small posterior fossa, displacement of posterior fossa structures	Hydrocephalus, chiari malformation, neurosurgical intervention
Hemorrhage and dilatation fourth ventricle, small SDH	IVH grade 3, PHVD, neurosurgical intervention
Hemorrhage and dilatation fourth ventricle, small SDH	IVH grade 3, PHVD, neurosurgical intervention
Hemorrhage and dilatation fourth ventricle, small SDH	IVH grade 3, PHVD, neurosurgical intervention
Large extra axial hemorrhage with compression on right cerebellar hemisphere, fourth ventricle and brain stem	Abnormal neurologic exam
Large extra axial haemorrhage, compression cerebellar vermis, hemispheres, fourth ventricle and brain stem	Abnormal neurologic exam, neurosurgical intervention
(old) cerebellar hemorrhage with disruption cerebellar vermis and hemispheres	Intra uterine transfusions for haemolytic disease
Normal	Group B streptococcal meningitis

IVH=intraventricular haemorrhage, PHVD=post hemorrhagic ventricular dilatation, SDH=subdural haemorrhage.

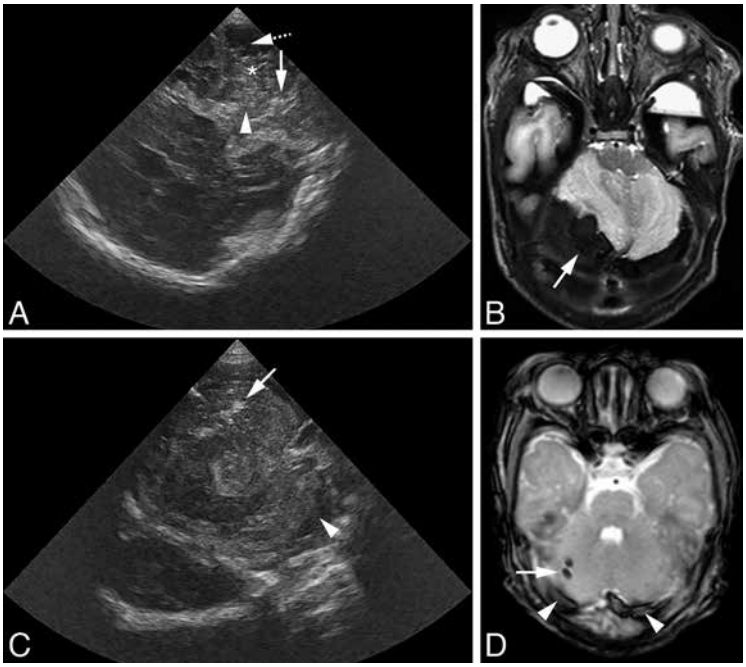

Figure 1. Male infant born at 37 weeks gestational age after precipitous labour. Abnormal neurologic examination and respiratory failure developing in the first hours after birth.
(A) CUS scan (right MF) shows a large extra axial hemorrhage (dotted arrow) with mass effect on the right cerebellar hemisphere (asterix), shift of the vermis (arrow) and compression of fourth ventricle (arrowhead). **(B)** T2-weighted MRI in same infant confirms the presence of a large extra-axial posterior fossa hemorrhage (arrow) with mass effect on the cerebellum and brain stem. Emergent neurosurgical decompression was performed and the boy fully recovered.

Male infant born asphyxiated at 39 weeks gestational age after non-assisted vaginal delivery.
(C) Cranial US (5th postnatal day, right MF) shows small focal echogenic lesions in right cerebellar hemisphere (arrow), suspect for hemorrhages and small extra-axial hemorrhage surrounding left cerebellar hemisphere (arrowhead). **(D)** T2*-weighted MRI (7th postnatal day) confirms small cerebellar hemorrhages in right hemisphere (arrow) and small extra axial posterior fossa hemorrhage (arrowheads).

In 12 infants minor abnormalities were diagnosed on both MF-CUS and MRI: punctate cerebellar hemorrhage (1 infant) (Figure 1), small extra-axial hemorrhage (9 infants) and mildly enlarged cisterna magna (2 infants).

In 2 infants the abnormalities suspected on MF-CUS were not confirmed by MRI. One infant with meningitis showed increased echogenicity and loss of foliation of

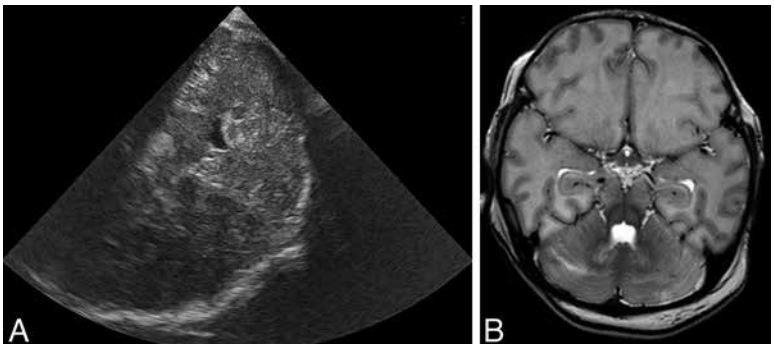

Figure 2. Female infant, born at 37 weeks gestational age, with severe perinatal asphyxia.
(A) MF-CUS on 5th postnatal day shows diffuse increased echogenicity of the cerebellum with loss of normal appearance of cerebellar foliae. **(B)** T2-weighted MR image on same day shows abnormal signal intensity in both cerebellar hemispheres with loss of normal foliation. Also showing extensive supratentorial abnormalities.

both cerebellar hemispheres (classified as major, Table 2) on MF-CUS, possibly representing edema. The MRI scan that was performed 8 days later showed no abnormalities. In the other infant a minor extra axial hemorrhage was suspected on MF-CUS, but this was in retrospect, a misinterpretation of a scanning artifact and might have been avoided when both MF had been used. In 1 infant a cerebellar hemorrhage was suspected on the AF only, but this finding was not confirmed by MRI.

MRI findings in infants with normal CUS findings

MRI detected abnormalities in 32 infants with normal CUS findings. In 7 infants these abnormalities were classified as major/clinically relevant (Table 3): in 4 infants with HIE, MRI showed SI changes of the cerebellar vermis, which were only seen on the diffusion-weighted images (Figure 5); in 1 infant with allo-immune thrombocytopenia, T2* MRI sequences showed a hemorrhagic lesion in the cerebellar vermis, probably of fetal origin; 1 infant had cerebellar dysplasia with abnormal foliation which was, in retrospect, also visible on MF-CUS; and 1 infant had a small arachnoid cyst in the cerebellopontine angle, which could not be visualized on the MF views. The other 25 infants had minor PF abnormalities, including punctate cerebellar hemorrhage (3 infants), small extra axial hemorrhages (18 infants), and combined punctate cerebellar hemorrhage and small extra axial hemorrhage (4 infants).

Table 3. Major MRI findings in infants with normal cranial ultrasound findings

Infant no.	GA	Category	MF-CUS	MRI	Other diagnoses
33	41	HIE	Small SDH	Abnormal SI cerebellar vermis (*), small SDH	
34	41	HIE	No posterior fossa abnormalities	Abnormal SI vermis (*)	
35	39	HIE	No posterior fossa abnormalities	Abnormal SI vermis (*)	Died
36	36	HIE	No posterior fossa abnormalities	Abnormal SI vermis (*)	Died
37	39	Malformation	No posterior fossa abnormalities	Cerebellar dysplasia with abnormal foliation	Aicardi syndrome
38	36	Hemorrhage	No posterior fossa abnormalities	(Old) vermian hemorrhage without atrophy	Neonatal alloimmune thrombocytopenia, supratentorial parenchymal hemorrhage
39	38	Malformation	No posterior fossa abnormalities	Small arachnoid cyst in right cerebellopontine angle	Aicardi syndrome

GA=gestational age, MF-CUS=mastoid fontanelle cranial ultrasound, HIE=hypoxic-ischemic encephalopathy, CNS=central nervous system, SDH=subdural hemorrhage.
(*) Abnormal signal intensity (SI) only detected on diffusion-weighted MRI.

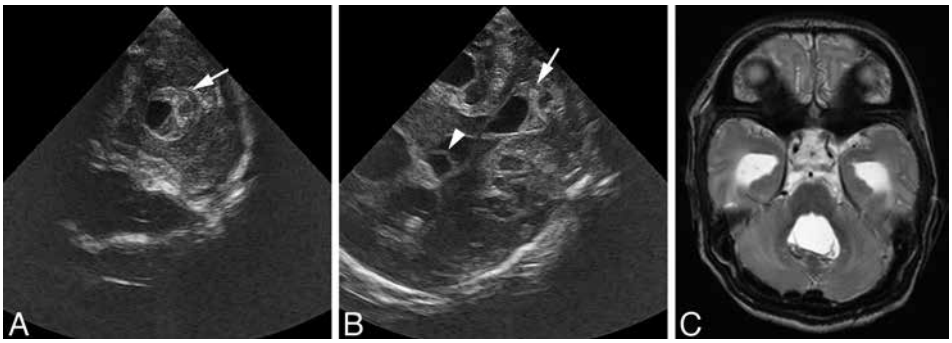

Figure 3. Male infant born at 41 weeks gestational age, admitted at 8th postnatal day with E. Coli meningitis and symptoms of increased intracranial pressure. CUS scan though AF showed severe ventricular dilatation (not shown).
(A) Axial and **(B)** coronal US through MF shows debris in dilated fourth ventricle (arrow) and strands in third ventricle (arrowhead). **(C)** T2-weighted MRI confirms CUS findings.

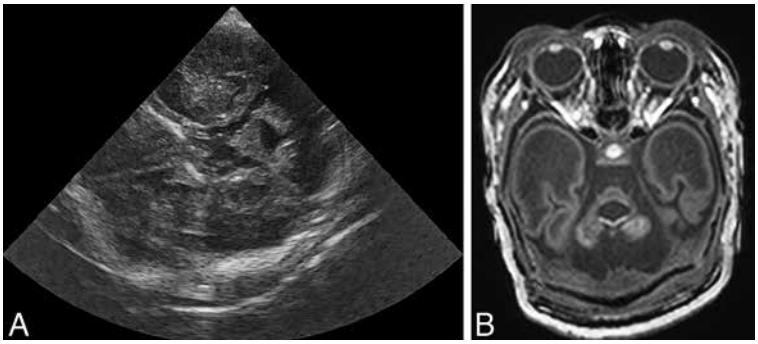

Figure 4. Male infant born at 38 weeks gestation who died in the neonatal period. Fetal polyhydramnios, neonatal hypotonia, contractures and respiratory failure. Suspected type IV 3-Methylglutaconic aciduria. CUS scan with AF as acoustic window showed a dilated ventricular system with abnormal echogenicity of the basal ganglia and abnormal gyral pattern.
(A) Axial CUS scan though MF shows severe hypoplasia of cerebellum and pons, with enlarged fourth ventricle and pericerebellar spaces. **(B)** T1-weighted MRI confirms severely hypoplastic cerebellum and pons. Gyral abnormalities of the temporal lobes can be seen on this image.

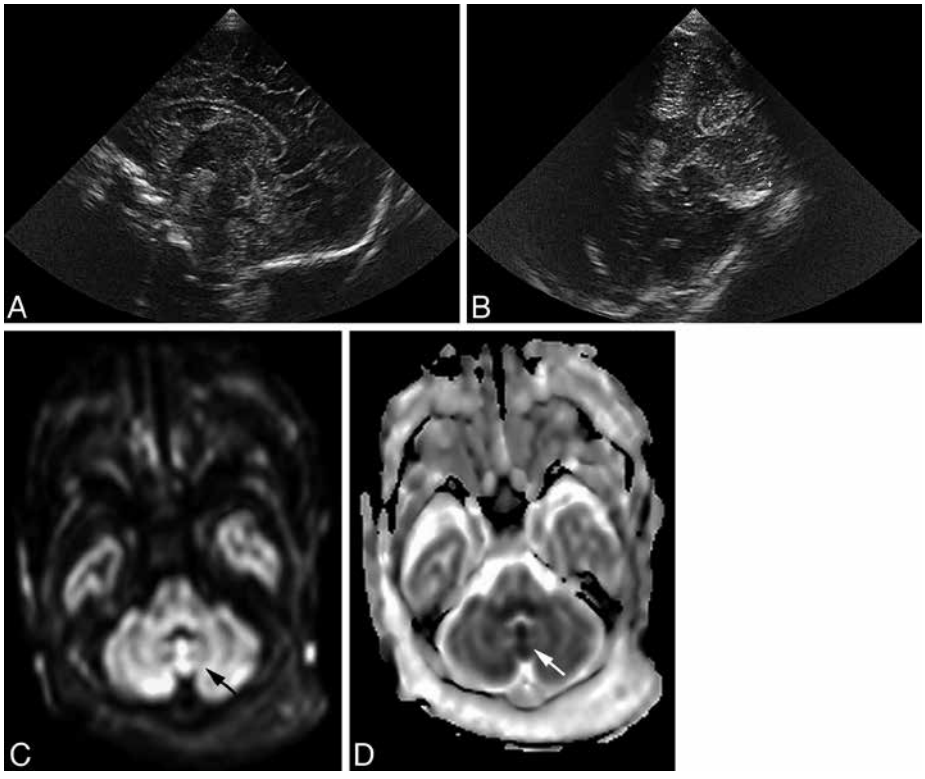

Figure 5. Female infant born at 39 weeks gestational age with severe perinatal asphyxia.
CUS on 3rd postnatal day with normal appearance of the cerebellar vermis on the midsagittal **(A)** and MF **(B)** views. **(C)** Diffusion-weighted MRI on 6th postnatal day shows diffusion restriction in the cerebellar vermis (arrow) with corresponding low signal on the ADC map (Figure (B) arrow).

Predictive values of CUS

The sensitivity and specificity of routine AF-CUS views for major/clinically relevant PF abnormalities, as seen on MRI, were 16% and 99%, and the positive and negative predictive values 86% and 70%, respectively. Adding the MF views increased the sensitivity of CUS for major/clinically relevant PF abnormalities to 82% and the positive and negative predictive values to 97% and 91%, respectively.

The sensitivity and specificity of CUS with additional MF views for the detection of any (major or minor) PF abnormality, as seen on MRI, were 57% and 95%. The positive predictive and negative predictive values were 96% and 53%, respectively.

Discussion

This is the first study assessing the prevalence of PF abnormalities in high-risk term infants and comparing the diagnostic accuracy of CUS, including both AF and MF views, with MRI.

MRI detected PF abnormalities among 75 (66%) of the 113 infants in our cohort of high-risk term infants; in 38 (34%) of the infants these abnormalities were classified as major and clinically relevant. The majority (82%) of major/relevant abnormalities were also found on MF views, but remained undetected when only AF views were used. In 7 infants, MRI demonstrated clinically relevant PF abnormalities that remained undetected on MF views.

Our results indicate that the addition of MF views to standard AF-CUS is an essential early diagnostic tool in high-risk term infants. Due to practical shortcomings, such as transportation of the neonate, MRI can be undesirable or unfeasible during the first days after birth, especially in critically ill neonates. MF-CUS detects the majority of clinically relevant PF abnormalities much earlier than possible with MRI.

The high percentage of infants with PF abnormalities in this study (66%) is probably secondary to the inclusion of both major and minor abnormalities in a high-risk population. Furthermore, we used diffusion-weighted images to detect acute hypoxic-ischemic injury and T2* sequences that are especially sensitive for the detec-

tion of small hemosiderin deposits (18). In addition, T1- and T2-weighted images had a slice thickness of 1 and 2 mm respectively, thereby assuring the detection of even the smallest lesions.

The most frequent major abnormality was diffuse echogenicity and/or SI change in the cerebellar parenchyma in cases with severe HIE. Among the 51 infants with HIE, 13 (25%) of the infants had parenchymal abnormalities on MRI; in 9 of them these abnormalities were also identified on MF-CUS. These 13 infants had a higher mortality (8/13 (62%)) than the whole group of infants with HIE (13/51 (26%)), suggesting that infants with HIE and cerebellar involvement were more severely affected. Although sparing of the cerebellum in term infants with HIE has been reported (19-21), the cerebellum can be involved in hypoxic-ischemic injury (22). This is further supported by neuroimaging studies using late or follow-up MR scans describing involvement of the cerebellum, specifically the vermis, in HIE (23-25). Autopsy and combined autopsy/MR studies also showed the cerebellum to be frequently involved in infants with severe hypoxic-ischemic injury (26,27).

Another common major abnormality was cerebellar hypoplasia, which was seen in 6 infants, 5 of whom had various inborn errors of metabolism. All cases were detected on MF views. Several inborn errors of metabolism can affect early cerebellar development (6,7) and lead to cerebellar hypoplasia or atrophy. In combination with a clinical picture suggesting a metabolic disorder, this finding on CUS may help diagnosing the underlying disease.

There were 8 infants with significant PF hemorrhage, of whom 7 were diagnosed on MF views. In 4 infants with fourth ventricular or large extra axial posterior fossa hemorrhages, neurosurgical intervention was needed because of brain stem compression or progressive ventricular dilatation. Two infants had large parenchymal cerebellar hemorrhages that resulted in cerebellar atrophy on follow-up studies. A previous study in term infants showed that these large hemorrhages are associated with a broad spectrum of neurodevelopmental disabilities (2).

The most common minor abnormalities seen were small extra axial hemorrhages in 38 (34%) and punctate cerebellar hemorrhages in 10 (9%) of the 113 infants of this high-risk population. Previous studies have shown that small extra axial hemorrhages are a common MRI finding in asymptomatic term newborns. Looney et al.

(16) reported a prevalence of 26% of asymptomatic intracranial hemorrhages on MRI after vaginal birth in full-term infants, the majority were subdural and infratentorial hemorrhages. Rooks et al. (17) reported an incidence of 20% of PF subdural hemorrhages in asymptomatic term infants. Most hemorrhages resolved spontaneously within one month and did not affect neurodevelopmental outcome at 2 years. Punctate cerebellar hemorrhages are a common MRI finding in very preterm infants (15,28) and have a favorable outcome (15). Not much is known about the incidence and consequences of punctate cerebellar hemorrhage in term infants. Our study suggests that these hemorrhages are also common in high-risk term infants.

Our study has a few limitations. Firstly, this was a selective and retrospective cohort of high-risk term infants assessed with both MF-CUS and MRI. The true incidence of PF abnormalities in specific clinical conditions, such as HIE, metabolic disorders or CNS infection cannot be determined from our study and needs to be studied prospectively. Secondly, there was an interval between the CUS and MRI examinations. A prospective study with CUS and MRI performed on the same day may reveal a higher sensitivity of CUS, especially in cases with HIE (29,30) or CNS infection. Finally, CUS examination is operator dependent. Increasing experience with the MF approach will improve knowledge of the normal anatomy and imaging appearance of the PF and lead to an increased detection of abnormalities. However, all CUS scans in this study were performed by well-trained neonatology staff members.

In conclusion, we found a high prevalence of PF abnormalities in high-risk term infants. MF-CUS enables early diagnosis of the majority of major and clinically relevant PF abnormalities. We therefore propagate to routinely perform MF-CUS not only in preterm, but also in high-risk term neonates.

References

1. Limperopoulos C, Bassan H, Gauvreau K, et al. Does cerebellar injury in premature infants contribute to the high prevalence of long-term cognitive, learning, and behavioral disability in survivors? Pediatrics 2007; 120:584-593.
2. Limperopoulos C, Robertson RL, Sullivan NR, Bassan H, du Plessis AJ. Cerebellar injury in term infants: clinical characteristics, magnetic resonance imaging findings, and outcome. Pediatr Neurol 2009; 41:1-8.
3. Steggerda SJ, de Bruine FT, Smits-Wintjens VE, Walther FJ, van Wezel-Meijler G. Ultrasound detection of posterior fossa abnormalities in full-term neonates. Early Hum Dev 2012; 88:233-239.
4. Miall LS, Cornette LG, Tanner SF, Arthur RJ, Levene MI. Posterior fossa abnormalities seen on magnetic resonance brain imaging in a cohort of newborn infants. J Perinatol 2003; 23:396-403.
5. Volpe. Neurology of the newborn. (ed. 5). Philadelphia: Saunders, 2008.
6. Steinlin M, Blaser S, Boltshauser E. Cerebellar involvement in metabolic disorders: a pattern-recognition approach. Neuroradiology 1998; 40:347-354.
7. Leijser LM, de Vries LS, Rutherford MA, et al. Cranial ultrasound in metabolic disorders presenting in the neonatal period: characteristic features and comparison with MR imaging. AJNR Am J Neuroradiol 2007; 28:1223-1231.
8. Steggerda SJ, Leijser LM, Walther FJ, van Wezel-Meijler G. Neonatal cranial ultrasonography: how to optimize its performance. Early Hum Dev 2009; 85:93-99.
9. Correa F, Enriquez G, Rossello J, et al. Posterior fontanelle sonography: an acoustic window into the neonatal brain. AJNR Am J Neuroradiol 2004; 25:1274-1282.
10. Enriquez G, Correa F, Aso C, et al. Mastoid fontanelle approach for sonographic imaging of the neonatal brain. Pediatr Radiol 2006; 36:532-540.
11. Di Salvo DN. A new view of the neonatal brain: clinical utility of supplemental neurologic US imaging windows. Radiographics 2001; 21:943-955.
12. Steggerda SJ, Leijser LM, Wiggers-de Bruine FT, van der GJ, Walther FJ, van Wezel-Meijler G. Cerebellar injury in preterm infants: incidence and findings on US and MR images. Radiology 2009; 252:190-199.
13. Meijler G. Neonatal Cranial Ultrasonography. 2nd ed: Springer Berlin Heidelberg, 2012.
14. van Wezel-Meijler G, Leijser LM, de Bruine FT, Steggerda SJ, van der GJ, Walther FJ. Magnetic resonance imaging of the brain in newborn infants: practical aspects. Early Hum Dev 2009; 85:85-92.
15. Steggerda SJ, de Bruine FT, van den Berg-Huysmans AA, et al. Small Cerebellar Hemorrhage in Preterm Infants: Perinatal and Postnatal Factors and Outcome. Cerebellum 2013; 12:794-801.
16. Looney CB, Smith JK, Merck LH, et al. Intracranial hemorrhage in asymptomatic neonates: prevalence on MR images and relationship to obstetric and neonatal risk factors. Radiology 2007; 242:535-541.
17. Rooks VJ, Eaton JP, Ruess L, Petermann GW, Keck-Wherley J, Pedersen RC. Prevalence and evolution of intracranial hemorrhage in asymptomatic term infants. AJNR Am J Neuroradiol 2008; 29:1082-1089.
18. de Bruine FT, Steggerda SJ, van den Berg-Huysmans AA, et al. Prognostic value of gradient echo T2* sequences for brain MR imaging in preterm infants. Pediatr Radiol 2014; 44:305-312.

19. Rutherford M, Ward P, Allsop J, Malamatentiou C, Counsell S. Magnetic resonance imaging in neonatal encephalopathy. Early Hum Dev 2005; 81:13-25.
20. Triulzi F, Parazzini C, Righini A. Patterns of damage in the mature neonatal brain. Pediatr Radiol 2006; 36:608-620.
21. Vermeulen RJ, Fetter WP, Hendrikx L, Van Schie PE, van der Knaap MS, Barkhof F. Diffusion-weighted MRI in severe neonatal hypoxic ischaemia: the white cerebrum. Neuropediatrics 2003; 34:72-76.
22. Martinez-Biarge M, Diez-Sebastian J, Kapellou O, et al. Predicting motor outcome and death in term hypoxic-ischemic encephalopathy. Neurology 2011; 76:2055-2061.
23. Sargent MA, Poskitt KJ, Roland EH, Hill A, Hendson G. Cerebellar vermian atrophy after neonatal hypoxic-ischemic encephalopathy. AJNR Am J Neuroradiol 2004; 25:1008-1015.
24. Le Strange E, Saeed N, Cowan FM, Edwards AD, Rutherford MA. MR imaging quantification of cerebellar growth following hypoxic-ischemic injury to the neonatal brain. AJNR Am J Neuroradiol 2004; 25:463-468.
25. Connolly DJ, Widjaja E, Griffiths PD. Involvement of the anterior lobe of the cerebellar vermis in perinatal profound hypoxia. AJNR Am J Neuroradiol 2007; 28:16-19.
26. Jouvet P, Cowan FM, Cox P, et al. Reproducibility and accuracy of MR imaging of the brain after severe birth asphyxia. AJNR Am J Neuroradiol 1999; 20:1343-1348.
27. Alderliesten T, Nikkels PG, Benders MJ, de Vries LS, Groenendaal F. Antemortem cranial MRI compared with postmortem histopathologic examination of the brain in term infants with neonatal encephalopathy following perinatal asphyxia. Arch Dis Child Fetal Neonatal Ed 2013; 98:F304-309.
28. Tam EW, Rosenbluth G, Rogers EE, et al. Cerebellar hemorrhage on magnetic resonance imaging in preterm newborns associated with abnormal neurologic outcome. J Pediatr 2011; 158:245-250.
29. Epelman M, Daneman A, Kellenberger CJ, et al. Neonatal encephalopathy: a prospective comparison of head US and MRI. Pediatr Radiol 2010; 40:1640-1650.
30. Daneman A, Epelman M, Blaser S, Jarrin JR. Imaging of the brain in full-term neonates: does sonography still play a role? Pediatr Radiol 2006; 36:636-646.